Food Hydrocolloids for Health 1 (2021) 100030

Contents lists available at ScienceDirect

Food Hydrocolloids for Health

journal homepage: www.elsevier.com/locate/fhfh

A detailed microstructural and multiple responses analysis through blocking design to produce Ca(II)-alginate beads loaded with bioactive compounds extracted from by-products

Tatiana Rocio Aguirre-Calvo [a,b], Daniel Aguirre-Calvo [c,d], Mercedes Perullini [c,d,*], Patricio R. Santagapita [a,b,*]

[a] Universidad de Buenos Aires, Facultad de Ciencias Exactas y Naturales, Departamento de Química Orgánica y Departamento de Industrias, Buenos Aires, Argentina
[b] CONICET-Universidad de Buenos Aires, Centro de Investigación en Hidratos de Carbono (CIHIDECAR), Buenos Aires, Argentina
[c] Universidad de Buenos Aires, Facultad de Ciencias Exactas y Naturales. Departamento de Química Inorgánica, Analítica y Química Física. Buenos Aires, Argentina
[d] CONICET-Universidad de Buenos Aires. Instituto de Química Física de los Materiales, Medio Ambiente y Energía (INQUIMAE). Buenos Aires, Argentina

ARTICLE INFO

Keywords:
Antioxidants
Waste
Hydrogels
Response surface methodology
SAXS

ABSTRACT

The aim of the present research was to optimize the generation of Ca(II)-alginate beads containing extracts from by-products using a blocking design, with a concomitant evaluation of the microstructural changes of the hydrogel network assessed by SAXS. Two main industrial parameters were used as variables: sodium-alginate and calcium-chloride concentrations. Multiple responses related to the loading efficiency of the bioactive compounds, their activity by two methods (ABTS and FRAP) and a macroscopic property (roundness) were analyzed through the experimental design. The blocking design was efficient compared to a randomized design as confirmed by F-value>1, highlighting the differences among the extracts. Besides, both synthesis variables significantly affected each response, showing the concentration of sodium alginate a higher impact. On the other hand, the extracts increased the interconnectivity of the rods (changing the fractal dimension from ~1.80 to ~2.10) due to the presence of trivalent cations since they induce a larger coordination of the network. The compactness and size of the rods and the characteristic size of the dimers were more influenced by the extracts than by the increase of alginate and calcium concentrations. The optimized combination of alginate (1.5% w/v) and calcium (2.5% w/v) achieved two goals: highest loading efficiency and activities of bioactive compounds, and stabilization of the microstructural modulations due to extract changes.

1. Introduction

Sodium alginate is a natural ionic polysaccharide typically extracted from the cell wall of brown algae, brown seaweed, and bacteria (Agüero, Zaldivar-Silva, Peña & Dias, 2017). The ability to undergo an almost temperature-independent sol/gel transition in presence of some bi or trivalent cations (e.g. Ca^{2+}, Sr^{2+}, Ba^{2+}, Al^{3+}, Ce^{3+}) (Dodero et al., 2019; Posbeyikian et al., 2021; Sonego, Santagapita, Perullini & Jobbágy, 2016) is widely used to prepare hydrogels. The gelation process is conventionally described in terms of the "egg-box" model, where ionic cross-linking interaction occurs between the carboxylic acid groups of alginate and cations, being a fast, simple, and mild-condition process, featuring qualities that make alginate a suitable choice as an encapsulation agent (Bennacef, Desobry-Banon, Probst & Desobry, 2021). As the concentration of alginate increases in the formulation, the number of apparent cross-linking points also increases (Kaur, Singh & Sharma, 2018). Calcium is the main divalent cation widely used due to being clinically safe, easily accessible, and economical (Reis, Neufeld, Vilela, Ribeiro & Veiga, 2006). Therefore, the control of the concentrations of sodium alginate and calcium may involve the optimization of the synthesis process entailing to enhance desired characteristics for a certain product. Additionally, analysis of the nanostructure and morphology of the associations of alginate chains have been conducted by SAXS revealing the different scales and arrangements within Ca(II)-alginate beads; the presence of natural extracts prompts important structural changes in the alginate network, from the molecular (arrange of alginate polymer dimers) to the supramolecular (interconnection of the rods composing the microstructure of the hydrogel) level (Aguirre Calvo, Perullini & Santagapita, 2018, 2019).

By-products of fruits and vegetables represent a source of sugars, minerals, organic acids, colorants, and phenolic compounds, that usually represent large amounts of wastes. Therefore, the recovery of

* Corresponding authors.
E-mail addresses: mercedesp@qi.fcen.uba.ar (M. Perullini), patricio.santagapita@qo.fcen.uba.ar, prs@di.fcen.uba.ar (P.R. Santagapita).

https://doi.org/10.1016/j.fhfh.2021.100030
Received 23 April 2021; Received in revised form 11 August 2021; Accepted 17 September 2021

these valuable compounds has gained significant economic interest as a good and cheap source of bioactive compounds, being also in line with United Nations Sustainable Development Goals (SDG) number 2 and 3 (United Nations, 2021). Besides, a wide range of benefits in humans was already documented, such as their important biological activities, including antioxidant, antibacterial, cardio-protective, anti-carcinogenic and anti-mutagenic effects (Brewer, 2011; Llorach, Espin, Tomás-Barberán & Ferreres, 2003; Shrikhande, 2000). To prevent undesirable changes in the properties of labile substances under adverse environmental conditions, encapsulation represents a very useful technique aimed to improve the stability and release of bioactive compounds such as food ingredients, enzymes, cells, or other materials by entrapping them within a coating agent or a matrix (Najafi-Soulari, Shekarchizadeh, & Kadivar, 2016; Stojanovic et al., 2012). Several researchers have been studying the versatility to encapsulate the bioactive in Ca(II)-alginate based matrices, contributing to an increase in stability and also promoting a controlled release of the bioactive compounds (Fang & Bhandari, 2010; Nedovic, Kalusevic, Manojlovic, Levic & Bugarski, 2011; Rijo et al., 2014). Previous works of our group demonstrated that the encapsulation of natural extracts into Ca(II)-alginate systems (commonly in the form of beads) provides advantages that contribute to the development of ingredients for functional foods (T. R. Aguirre Calvo, Molino, Perullini, Ruffian-Henares & Santagapita, 2020b; Traffano-Schiffo, Calvo, Avanza & Santagapita, 2020, 2018). Furthermore, the microstructural stabilization of the beads allowed to elucidate and evaluate the changes not only related to the encapsulation process but also to the physical characteristics and release properties during operative conditions (T. R. Aguirre Calvo, Molino, Perullini, Ruffian-Henares & Santagapita, 2020a; Traffano-Schiffo et al., 2018; Zazzali, Aguirre Calvo, Ruíz-Henestrosa, Santagapita & Perullini, 2019).

Response surface methodology (RSM) is known as a collection of statistical and mathematical techniques, useful for the development, improvement, and optimization of products and processes (Carley, Kamneva & Reminga, 2004; Deepak et al., 2008). By means of an RSM analysis, the combined effects of some factors involved in the beads production process can be evaluated, analyzing the influence and importance of independent variables to one or several dependent variables to improve a process and obtain an optimal response (Ji, Cho, Gu & Kim, 2007; Šumić et al., 2016). To the best of our knowledge, experiment design has been used focusing on some cases only in one or two responses of the Ca(II)-alginate matrices, such as encapsulation efficiency (Najafi-Soulari et al., 2016; Narsaiah, Jha, Wilson, Mandge & Manikantan, 2014), encapsulation efficiency and loading capacity (Celli, Teixeira, Duke & Brooks, 2016), evaluation of crosslinking degree (Dodero et al., 2019), and encapsulation efficiency and drug release (Nayak, Das & Maji, 2012). While loading efficiency allows to establish and optimize an encapsulation procedure, changes related to the physical properties of the beads are parameters that must also be considered, especially for fine-tuning the final application of them. Apart from performance parameters related to the quality and bioactivity of functional ingredients, additional desired properties are related to the acceptance of the beads in food systems, such as their sphericity (roundness), being key factors responsible for the appearance and texture of the product (Ha, Jo, Cho & Kim, 2016; Jeong, Kim, Lee, Cho & Kim, 2020). Particularly, it has been suggested that roundness is an appropriate measure to differentiate spherical particles as a shape descriptor (Lee, Ravindra & Chan, 2013) as well as a possible indicator of acceptance by consumers (Velasco, Beh, Le & Marmolejo-Ramos, 2018). Hence, the aim of this work was to optimize the generation of Ca(II)-alginate beads containing extracts from beet by-products (leaves and stems) using a blocking design, with a concomitant evaluation of the microstructural changes of the hydrogel network from the molecular to the supramolecular scale (1–100 nm) assessed by SAXS. Two main industrial parameters were used as variables: sodium alginate and calcium chloride concentrations, which were related to multiple responses as loading efficiency of the bioactive compounds, their activity as well as the roundness of the beads. The optimized formulation was not only related to the maximum responses, but also considering the microstructural modulations due to the interaction of the extracts and the synthesis variables on the Ca(II)-alginate bead, being the first time that all these parameters are contemplated altogether.

Table 1
Experimental levels of the independent variables.

Factor	Name	Unit	Levels
X1	Na-alginate	% w/v	0.5 –1.5
X2	$CaCl_2$	% w/v	1–4
X3	Extract		Leaf – Stem - Mix

2. Materials and methods

2.1. Materials

Sodium alginate (Algogel 5540) from Cargill S.A. (San Isidro, Buenos Aires, Argentina), with mannuronate/guluronate (M/G) ratio of 0.6 and molecular weight of 1.97×10^5 g/mol. Calcium chloride ($CaCl_2$) from Laboratorios Cicarelli (Reagents S.A., San Lorenzo, Santa Fe, Argentina). Folin-Ciocalteau and sodium citrate from Biopack (Biopack, Zárate, Buenos Aires, Argentina), TPTZ and ABTS from Sigma (Sigma-Aldrich Co., Ltd., Saint Louis, USA).

2.2. Preparation of the extracts

Stems and leaves of *Beta vulgaris* were purchased in a local market, then scalded and homogenized in a blender. Three different purees (stems, leaves, and mix – 1:1 of the formers-) were obtained and then mixed with water (1:1.5) for 5 min at 20 °C; afterward, they were centrifuged at 6000 rpm for 30 min. Extracts were kept in the dark at 4 ± 1 °C until used. The extracts were characterized, and the main results are showed in Table S1 of the Supplementary File I.

2.3. Beads synthesis with bioactive extracts

Beads were prepared by ionotropic gelation according to the dropping method described previously (Aguirre Calvo et al., 2018; Traffano-Schiffo, Aguirre Calvo, Castro-Giraldez, Fito & Santagapita, 2017) following the experimental design commented in the next section. Briefly: sodium alginate (Na-alginate) solutions were prepared in each extract (leaf, stem, or mix) (0.5, 1.0 and 1.5% w/v) under gentle agitation at room temperature until complete dissolution. Calcium chloride ($CaCl_2$) solutions (1.0, 2.5 and 4.0% w/v) were prepared in 0.1 M acetate buffer pH 5.5. Each Na-alginate solution (2 mL) was dripped over 20 mL $CaCl_2$ solutions (stirred in an ice bath) at 6 cm by using a peristaltic pump (model BT50–1J-JY10, Baoding Longer Precision Pump Co, Ltd, China) at 9.0 ± 0.1 rpm. After beads generation, they were maintained for 5 min in $CaCl_2$ solution, and then they were washed 2 times with bidistilled cold water to remove free Ca^{2+}. Finally, beads were maintained at 4 °C until their use.

2.4. Experimental design

The response surface method was used to estimate the effect of three variables on five dependent responses ($L.E_{TPC}$; $R.A_{ABTS}$; $R.A_{FRAP}$; $L.E_{BC}$ and roundness). A complete randomized block design was built, taking the extract as a blocking factor, to control the optimal response of Na-alginate:$CaCl_2$ for each extract. Table 1 summarizes the experimental variables selected and the variation range. To validate the theoretical models, an additional experiment was carried out. The response surface is based on the model generated from the blocking design.

The experimental data were fitted to a second-order polynomial model to obtain the regression coefficients. Regression analysis was performed with Eq. (1):

$$Y_m = \beta_0 + \sum_{i=1}^{k} \beta_i X_i + \sum_{i=1}^{k} \beta_{ii} X_i^2 + \sum_{i=1}^{k} \sum_{j=i+1}^{k} \beta_{ij} X_i X_j \quad (1)$$

where Y_m is the dependent variable analyzed (Y_1-L.E_{TPC}; Y_2-R.A_{ABTS}, Y_3-R.A_{FRAP}, Y_4-L.E_{BC}, Y_5-roundness); β_0 is a constant coefficient; βi, βii and βij are the coefficients for linear, quadratic and interaction effect, respectively; and X_i and X_j are the independent variables. The linear terms analyze the effect of one factor at a time over the response studied, while the interaction terms evaluate the effect of two factors simultaneously. The quadratic terms investigate a non-linear response. The sign and magnitude of each significant factor in the quadratic equation denote its relative influence on the dependent response evaluated. At the same time, each response is transformed to obtain a normal distribution, in case it be needed. A totally randomized block experiment was designed in which the extract is used as a blocking factor. A total of 33 experiments were performed and are presented in Fig S1 of the Supplementary File. Multiple response optimization was analyzed by Design-Expert statistical software (Version 11.0, StatEase, Inc, Minneapolis, MN, USA). The average of three runs for the optimal point in each extract was conducted and introduced on the model for the point prediction following the criterion of desirability.

2.5. Dependent variables measurements

2.5.1. Loading efficiency of betacyanins (L.E_{BC})

L.E_{BC} was calculated with the protocol followed by Aguirre Calvo et al. (2018–2019). Particularly, beads were liquefied with sodium citrate (30 beads mix with 0.5 mL of 20% w/v sodium citrate). Spectra from the samples were obtained with a Jasco V-630 UV–VIS spectrophotometer (JASCO Inc., Maryland, USA) working from wavelengths of 300 to 800 nm.

2.5.2. Loading efficiency of total phenolic compounds (L.E_{TPC})

L.E_{TPC} was calculated with the protocol followed by Aguirre Aguirre Calvo et al. (2018)-2019). Briefly, beads were liquefied with sodium citrate and absorbance was read at 765 nm. Results were expressed as mg gallic acid/mL through a calibration curve following the Folin-Ciocalteau method.

2.5.3. Remaining activity by $ABTS^{\bullet+}$ radical (R.A_{ABTS})

R.A_{ABTS} was calculated with the protocol followed by Aguirre Aguirre Calvo et al. (2018)-2019). Particularly, beads were liquefied with sodium citrate. Then, absorbance was read at 735 nm and results were expressed as mg eq gallic acid (GAE)/mL following the ABTS protocol (Wootton-Beard & Ryan, 2011).

2.5.4. Remaining ability for reducing ferric (R.A_{FRAP})

The ferric reducing ability of the extract and beads was determined following the technique of Benzie and Strain (1996)), with a modification. Briefly, FRAP reagent was prepared using buffer acetate (0.3 M, pH= 3.6), TPTZ (10 mM in 0.04 M HCl) and $FeCl_3 \bullet 6\,H_2O$ (20 mM), were mixed together in a ratio of 10:1:1 (% v:v:v). An aliquot of the extract (40 μL) was mixed with 60 μL of water and 600 μL of freshly prepared reagent and incubated in the dark at 30 °C for 30 min and then read at 563 nm ($FR_{extract}$). For beads, 10 beads were mix with FRAP reagent and incubated in the dark at 30 °C for 30 min, also read at 563 nm (FR_{beads}). The ferric reducing ability was calculated against a control (water or blank beads), compared to a gallic acid standard curve and expressed as mg eq gallic acid (GAE)/mL. The remaining activity was calculated:

$$R.A_{(FRAP)} = \left(\frac{[FR]_{beads}}{[FR]_{extract}} \right) * 100\ \% \quad (2)$$

2.5.5. Roundness

The shape of the beads was analyzed through digital analysis of images captured by a digital camera (Canon digital camera, 3.2 Mpix PowerShotA70; Canon Inc., Malaysia; with zoom fixed at 3x) coupled to a binocular microscope (Unitron MS, Unitron Inc., New York, USA, magnification at 7x) and analyzed by the free license software ImageJ (http://rsbweb.nih.gov/ij/), as described by Aguirre Calvo and Santagapita (2016) and Zazzali et al., 2019. Roundness gives an idea of how far the shape is from sphericity, by relating the area and the major axis of the bead. The equation that the software used to determine the roundness is: 4*area/(π*major_axis^2). At least 50 beads were analyzed by applying the "analyze particle" command of the software. The ImageJ software was calibrated to transform the measured pixels in length units (mm) by taking pictures of a caliper section.

2.6. Microstructural analysis

Microstructural parameters were analyzed as described in previous works (Aguirre Calvo et al., 2020a; Traffano-Schiffo, Calvo, Avanza and Santagapita, 2020; Traffano-Schiffo et al., 2018). Beads formulated for each point of the experimental design were measured at the LNLS SAXS1 beamline in Campinas (Brazil) working at $\lambda = 0.1488$ nm with a vector (q) range of 0.142 $nm^{-1} < q < 5.035\ nm^{-1}$. The obtained parameters were the degree of interconnection of the alginate rods (α_1), the degree of compactness within the rods (α_2), the connectivity between the associated polymer chains that blend alginate dimers (α_3), the size related to the outer radius of the rods (R_1) and the size related to the outer radius of the basic units of polymer dimers (R_2). Statistical differences were assessed by one-way ANOVA with Tukey's post-test by using Prism 6.01 (GraphPad Software Inc., San Diego, CA, USA).

3. Results and discussion

3.1. Optimization for loaded bioactive compounds in Ca(II)-alginate beads

The optimization of the two main variables on the synthesis of Ca(II)-alginate systems loaded with antioxidants and betacyanin by RSM is an advantage as a decisive step for obtaining beads for their subsequent use as functional ingredients but employing the minimum of experimental tests. The effect of both Na-alginate and calcium chloride concentrations as formulation variables in three different extracts on the betacyanins (BC) and total phenolic compounds (TPC) content, antioxidant activities by ABTS and FRAP, and roundness (as macroscopic property) of Ca(II)-alginate beads was studied. Table 2 shows the regression coefficients for the model of each response and p-values adjusted to a quadratic model (p-value <0.0001). The correspondent ANOVA for each variable is included in Table S2 in the Supplementary Files. It is worth noting that to adjust the normality of the R.A_{ABTS} and L.E_{BC} responses, the use of transformations (power and square root, respectively) was required to obtain a normal distribution. The influence of the synthesis variables is especially clear in each of the obtained responses, particularly the concentration of sodium alginate (p <0.05 for each variable). In the case of calcium chloride concentration, it was an important factor and although for L.E_{TPC} response the linear regression does not present p <0.05, the quadratic term does. Table 2 also shows all responses with a significant relationship for the AB (Na-alginate:$CaCl_2$) interaction, indicating an effect related to the interplay of both variables.

The blocking experiment provides a perfectly identifiable classification criterion that at the same time allows groups of experimental units to be made homogeneous with each other. The advantage lies in converting unplanned systematic variability into planned systematic variability (Goos & Donev., 2006). It is observed from Table S2 of the Supplementary File that using a blocking model was effective since in all the responses the variable "*extract*" shows a high sum of squares, which generates F-value > 1, indicating that blocking is efficient. At the same time, the loading efficiency of total phenolic content showed in Fig 1

Table 2
Regression coefficient table for the model of each response and p-values (in *italic* under each coefficient) from ANOVA analyzed via RSM.

Responses	Extract	intercept	A	B	AB	A^2	B^2
$L.E_{TPC}$	*leaf*	6.93	15.67	11.48	−5.52		−1.17
	stem	12.79	*0.0292*	*0.6581*	*<0.0001*		*0.0002*
	mix	14.42					
$(R.A_{ABTS})^{2,55}$	*leaf*	3925	569	2462	−2435	6016	−134
	stem	−1108	*<0.0001*	*<0.0001*	*<0.0001*	*<0.0001*	*0.3038*
	mix	939					
$R.A_{FRAP}$	*leaf*	−3.52	16.55	10.73	−1.91		−1.55
	stem	−3.44	*<0.0001*	*<0.0001*	*<0.0001*		*<0.0001*
	mix	1.71					
$Sqrt(L.E_{BC})$	*leaf*	−0.67	5.05	1.23	−0.38	−1.68	−0.14
	stem	2.73	*<0.0001*	*<0.0001*	*<0.0001*	*<0.0001*	*<0.0001*
	mix	1.28					
Roundness	*leaf*	0.60	0.426	0.029 *0.0360*	−0.024	−0.134	
	stem	0.59	*<0.0001*		*0.1410*	*<0.0001*	
	mix	0.61					

(A: Na-alginate concentration and B: calcium chloride concentration).

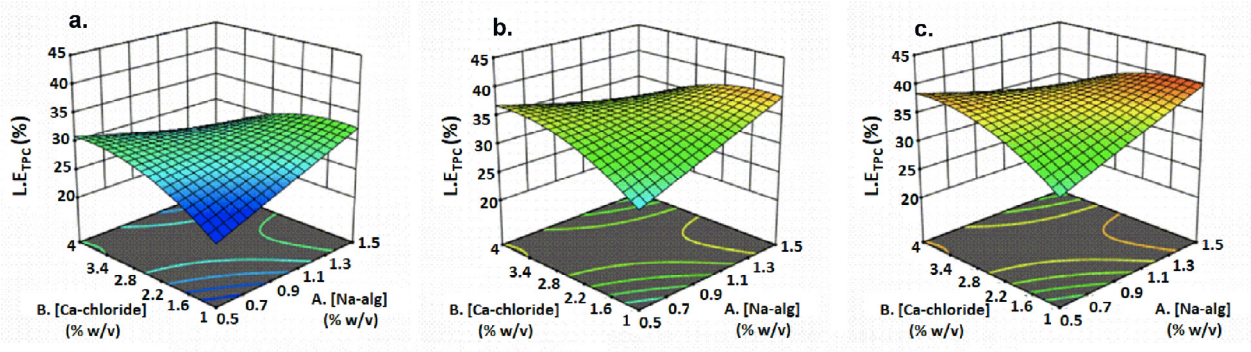

Fig. 1. Surface responses plots for the response of loading efficiency of total phenolic content ($L.E_{TPC}$) as a function of the sodium alginate concentration and calcium chloride concentration, for the by-product beet extracts of Ca(II)-alginate beads. **a**. Leaf **b**. Stem **c**. Mix. Please see Supplementary II, Fig S4 for animation of this figure.

reveals that each extract is represented at a different level in the same response surface (i.e. same function), demonstrating the effectiveness of the blocking experiment.

Fig.1 also shows that the minimum loading efficiency for TPC corresponds to low concentrations of both Na-alginate and calcium chloride. This behavior is closely related to the surface graphs that are presented for $R.A_{ABTS}$, $R.A_{FRAP}$, and $L.E_{BC}$ in Fig. 2abc, indicating in each case the same trend: loading efficiencies are low when the concentrations for both Na-alginate and $CaCl_2$ are 0.5% and 1.0%. On the other hand, as can be observed in Fig. 2d, these synthesis conditions also generate low values of roundness. This can be understood from the competing effects to maintain the drop shape between the viscous–surface tension and impact-drag forces acting when an alginate liquid drop hits and enters the gelling bath (Chan, Lee, Ravindra & Poncelet, 2009). As the alginate concentration is increased, the encapsulation efficiency improves significantly, as confirmed by the significance of the Na-alginate variable in Table 2 for the ANOVA of each response. For a low alginate concentration (<1.0%), the viscous and surface tension forces are lower than the minimum ones required to counteract the effect of impact and drag, and almost no spherical particles are formed, probably due to the lack of enough carboxyl groups for gelation. This probably leads to higher diffusion rates from the beads to the external media, reducing loading efficiencies. In contrast, when sodium alginate concentration is higher, the viscosity of the aqueous phase increases, giving in larger droplets with a wide distribution (Liu et al. 2004).

Finally, regarding the effects attributable to the presence of the different extracts in the formulations, the leaf extract (Fig 1a) presents the lower $L.E_{TPC}$ response, which correlates with the response for $L.E_{BC}$ and $R.A_{FRAP}$ (Figs S2 of the Supplementary File). On the other hand, samples with stem and mix extracts presented higher levels for their loading efficiency responses (as shown in Fig. 2 and S3 of the Supplementary File, respectively). Similar loading encapsulation using the same extract was observed by Aguirre Calvo and co-workers (2018), generating beads with important antioxidant values that can be applied as ingredients in functional food. Considering other works, it is important to highlight that the loading efficiency also depends on the nature of the encapsulated molecule. Among the aqueous loaded compounds, Najafi-Soulari et al. (2016) also obtained lower values (between 5 and 31%) for an aqueous lemon balm extract rich in phenolic compounds; Narsaiah et al. (2014) between 20 and 39% for encapsulating nisin (a small, cationic, hydrophobic peptide used as antimicrobial), but also employing guar gum, which often increases the encapsulation efficiency. Finally, Nayak et al. (2012) obtained between 54 and 74% for glibenclamide (a sulfonylurea used for non-insulin dependent diabetes treatment), but they also add arabic gum in almost 1:1 proportion with respect to alginate.

3.2. Microstructural analysis for Ca(II)-alginate beads

The microstructure of the beads was analyzed by SAXS, a technique that has been widely used to characterize the specific fractal regions of the alginate gel structure, generating insight into the interactions with the encapsulated compounds or among components ((Aguirre Calvo et al., 2020a)Traffano-Schiffo et al., 2020; Traffano-Schiffo et al., 2018). The parameters are obtained by analyzing the log-log SAXS plots (representative samples are included in Fig S9 of the Supplementary File II as an example) allowing to fully understand the microstructure of the hydrogel for the Ca(II)-alginate network, from the rods-like struc-

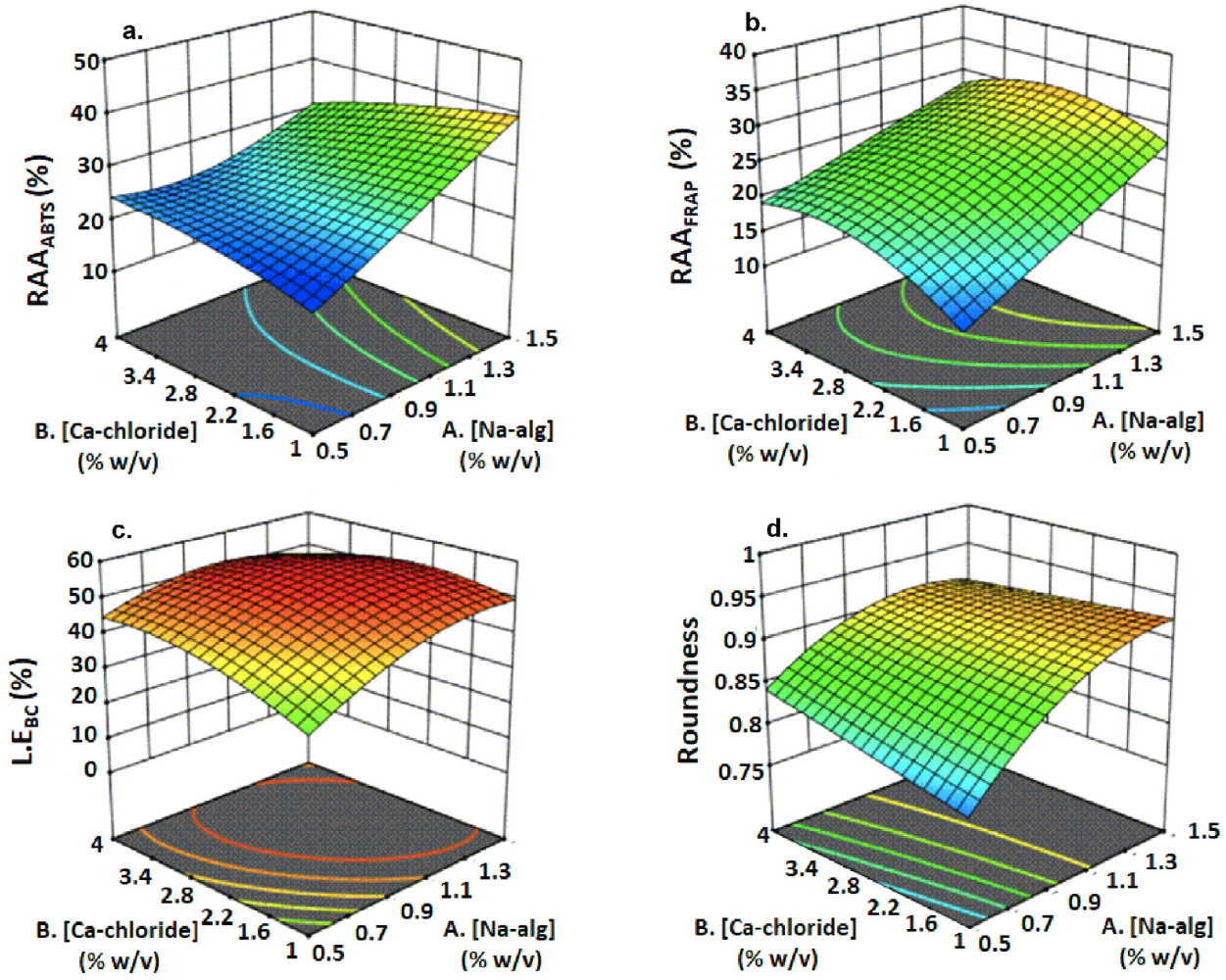

Fig. 2. Surface responses plots for **a.** remaining activity by ABTS radical ($R.A_{ABTS}$), **b.** remaining ability for reducing ferric ($R.A_{FRAP}$), **c.** loading efficiency of betacyanin ($L.E_{BC}$) and **d.** roundness as a function of the sodium alginate concentration and calcium chloride concentration, for the stem extract in the of Ca(II)-alginate beads. Figures for leaf and mix extracts are presented in Supplementary Figures S2 and S3 of Supplementary File I, respectively, and their animations in Figures S5-S8 of the Supplementary File II.

tures to the basic units (dimers) that built up those rods. Further insights into the gelling process can be found elsewhere (Bennacef et al., 2021; Zazzali et al., 2019).

The microstructure at the level of the basic structures (dimers) that self-associate to compose each of the rods in the alginate network is analyzed by parameters α_3 (density of dimers) and R_2 (characteristic size of dimers) and is presented in Fig 3. The presence of the extracts significantly affects the characteristic size of the basic structures (Fig 3B), generating dimers with higher sizes when any extract is added. Conversely, the density of the alginate dimers (Fig. 3A) does not present any trend (sustained increase or decrease) due to the addition of the extracts, agreeing with the results presented by Aguirre Calvo et al. (2018). When increasing the alginate concentration, beads with stem extract showed an increase both in the characteristic size of the dimers and in their compactness. This increase is also observed although to a lesser extent in the beads that have mix extract. Control beads presented an increase in the characteristic size of the dimers when increasing the alginate concentration, although this behavior is not seen in their compactness. No general trend is observed at this scale and for these parameters with the calcium concentration.

The compactness and size of the alginate rods are represented by parameters α_2 and R_1, respectively. Fig 4 shows that both parameters are influenced by the addition of the extracts and are less affected by the increase of alginate and calcium concentrations. Parameter α_2 takes values between 3.1–3.8, and leaf extract promotes the main effect observed in the compactness. This behavior is in line with previous works (Aguirre Calvo et al., 2018, 2019). A similar trend is observed for the size of the rods (R_1) that increases with the addition of extracts. This effect is attributed to the concentration of trivalent cations (mainly Fe^{3+}) that offer a more versatile and broad coordination environment (Sonego et al., 2016). The extract from beet by-products contained relevant concentrations of trivalent cations, in particular Fe^{3+}, which were more than 2 times higher in the leaf than in the stem extract (14. 4 ± 0.3 vs. 6.4 ± 0.6 mg Fe^{3+}/ kg sample, being the mix between them), in accordance with Aguirre Calvo et al., 2019. This same phenomenon is observed for the beads containing mix extract, although in a smaller proportion since this extract contains a portion of the leaf. On the other hand, a subtle modulation is found for the synthesis variables studied: as the alginate concentration increases, the compactness of the rods decreases, especially in the control samples, and there is a tendency to lower compactness for the lowest Ca^{2+} concentration (1.0%) which can be attributed to fewer and less extended junction zones.

Fig. 5 shows α_1 parameter, which reflects the fractal dimension at distances greater than the characteristic size of the rods that interconnect the structure of the alginate network. The addition of the extracts generates a network with greater compactness, particularly in the leaf extract, in comparison with those beads that do not have any extract (control). It has been demonstrated that the addition of the extract is a

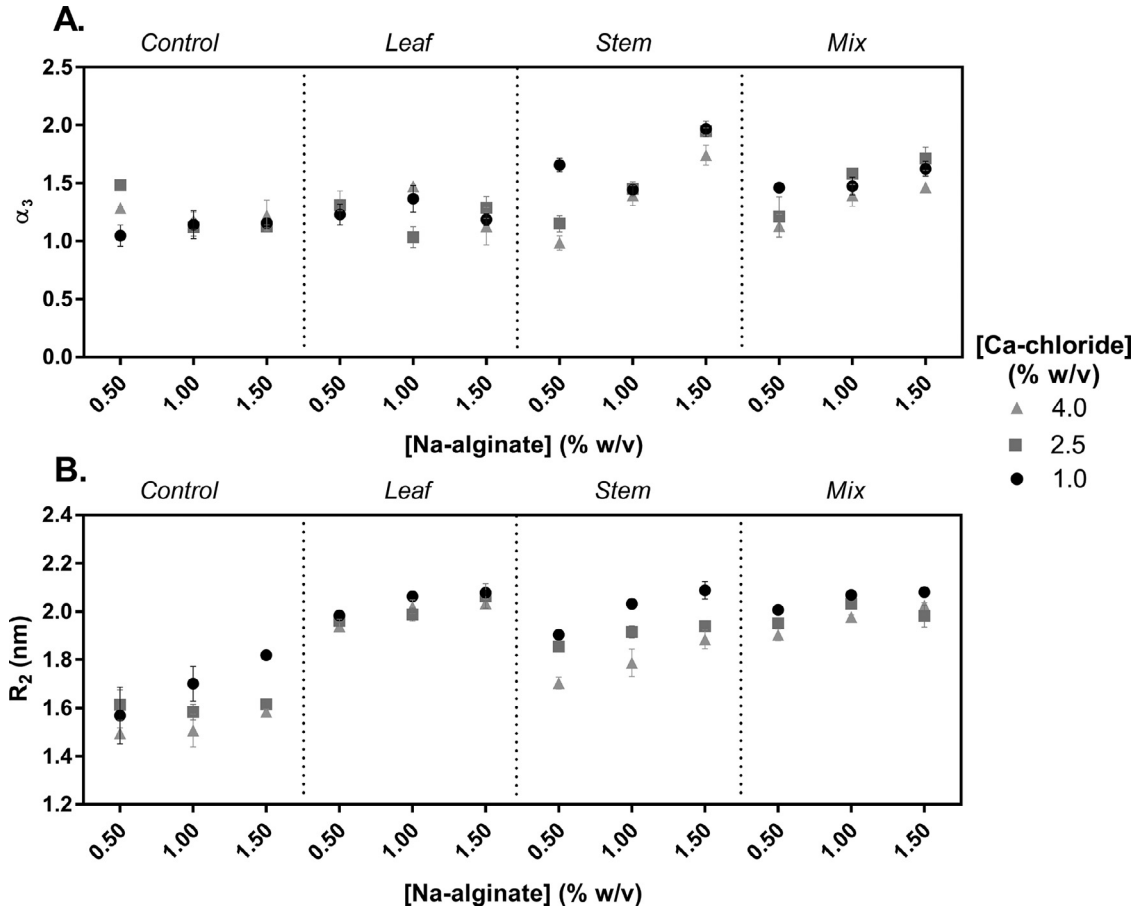

Fig. 3. Microstructural parameters for Ca(II)-alginate beads containing extracts (**leaf, stem,** and **mix**) as a function of the concentration of sodium alginate and calcium chloride. Control Ca(II)-alginate beads without extract were also included for comparative purposes. **A.** Parameter α_3 corresponding to the fractal dimension at distances lower than the size of the dimers derived from log–log SAXS profiles. **B.** Parameter R_2 as the characteristic size of the Ca(II)-alginate dimers deduced from the minima obtained on Kratky plots. Standard deviation values are included.

Table 3
Predicted and experimental values obtained for the validation of the regression model in the design.

Na-alginate (% w/v)	Calcium chloride (% w/v)	Extract		L. $E._{TPC}$	$R.A._{ABTS}$	$R.A._{FRAP}$	$L.E._{BC}$	Roundness	Desirability
1.5	2.5	Mix	Predicted	38.62	39.15	36.53	33.75	0.926	0.85
			Experimental	35.18	40.07	37.3	32.95	0.945	
			Error%	**9.8**	**2.3**	**2.1**	**2.4**	**2.0**	
1.5	2.5	Stem	Predicted	36.99	36.26	31.38	52.63	0.915	0.83
			Experimental	34.86	36.86	30.64	54.89	0.927	
			Error%	**6.1**	**1.6**	**2.4**	**4.1**	**1.3**	
1.5	2.5	Leaf	Predicted	31.17	42.89	31.29	14.88	0.925	0.81
			Experimental	29.67	43.24	33.23	15.44	0.932	
			Error%	**5.0**	**0.8**	**5.8**	**3.6**	**0.7**	

highly influential factor in generating a more interconnected structure in the alginate network (Aguirre Calvo et al., 2019; Traffano-Schiffo et al., 2020) due to the presence of trivalent cations. By incorporating Fe^{3+} ions, there is an incidence of tripartite nodes which generates a pre-established cross-linking in the alginate branches in solution producing triple coordination and therefore a higher level of disorder in the network, which increases the value of α_1. When the alginate concentration is increased, a dilution effect of the Fe^{3+} from the extract is reached. The Fe^{3+}/alginate ratio decreases, which also dilutes this triple knot effect that iron ions do. Increasing the alginate concentration reduces the degree of interconnection, which in turn decreases the fractal dimension of that network. On the other hand, at high concentrations of Na-alginate not only the effect of Fe^{3+} is diluted (as mentioned above), but also the concentration of Ca^{2+} has no significant effect. In this way, an interesting balance is observed: when there is a higher concentration of Fe^{3+} (pre-coordinating Na-alginate chains), α_1 changes significantly regardless of the concentration of Ca^{2+} ions in the cross-linking solution. With a higher concentration of cations, it is expected that finer rods will be quickly formed with the less alginate polymer present (as confirmed by R_1 values, Fig. 4B), and at the same time, these rods are expected to be more interconnected with the abundant Ca^{2+} present.

3.3. Validation

According to this design and with the goal of maximizing the phenolic compound content and their antioxidant activities, the betacyanin content and the roundness, the optimal combination of alginate and calcium for each extract with desirability > 0.8 (desirability plots and all the solutions for the optimization of the design are presented in Fig S10 and Table S3 in the Supplementary File II, respectively) is alginate

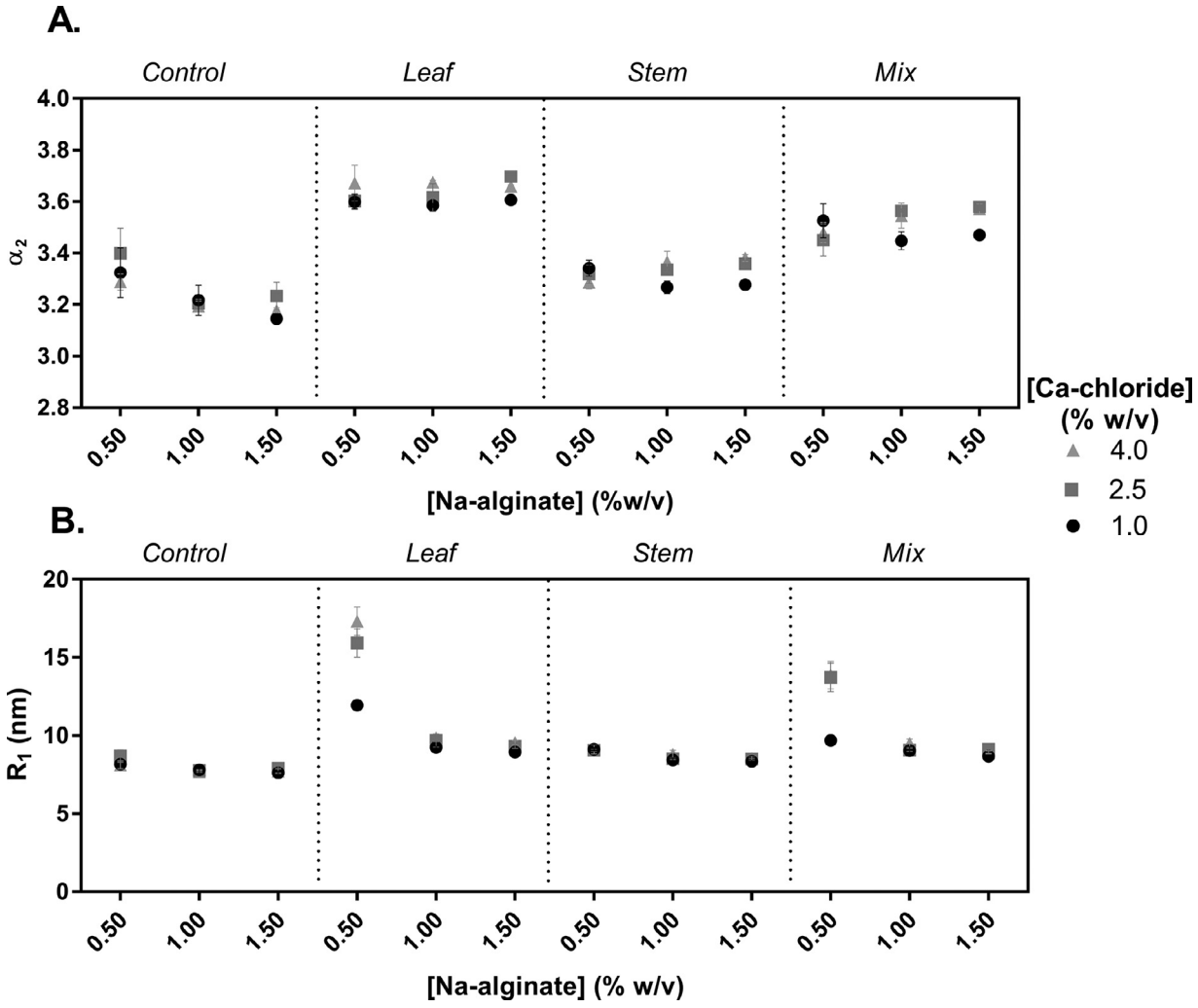

Fig. 4. Microstructural parameters for Ca(II)-alginate beads containing extracts (**leaf, stem,** and **mix**) as a function of the concentration of sodium alginate and calcium chloride. Control Ca(II)-alginate beads without extract were also included for comparative purposes. **A**. Parameter α_2 corresponding to the fractal dimension at distances lower than the characteristic size of the rods derived from log–log SAXS profiles. **B.** Parameter R_1 corresponding to the rod cross-sectional radius inferred from the maxima obtained on Kratky plots. Standard deviation values are included.

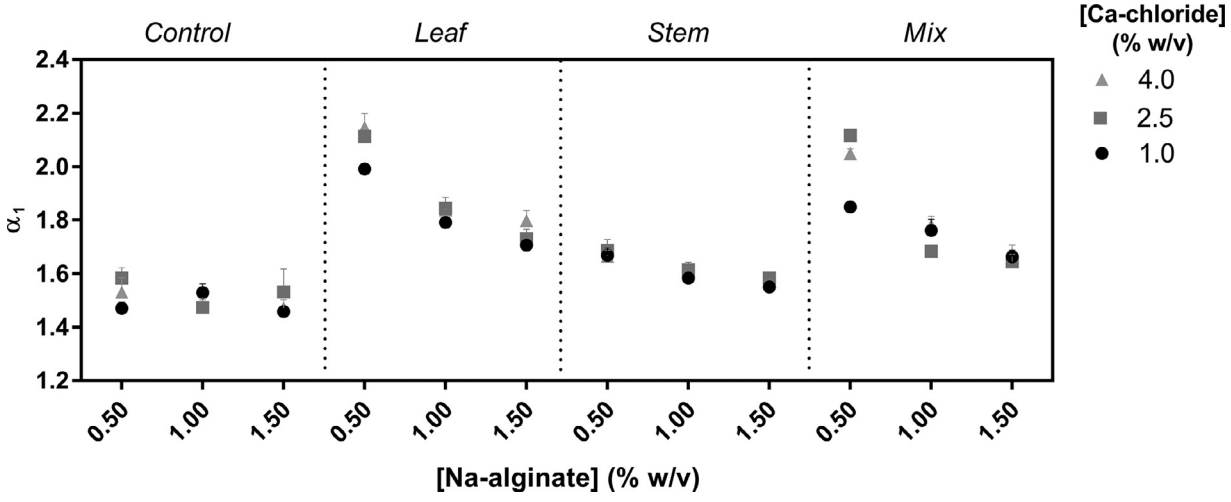

Fig. 5. Microstructural parameter α_1 corresponding to the fractal dimension of the alginate network derived from log–log SAXS profiles of Ca(II)-alginate beads containing extracts (**leaf, stem,** and **mix**) as a function of the concentration of sodium alginate and calcium chloride. Control Ca(II)-alginate beads without extract were also included for comparative purposes. Standard deviation values are included.

1.5% w/v and calcium 2.5% w/v, as shown in Table 3. After the confirmation, the experimental values were included in the model, being the difference between predicted and experimental values less than 6% (with an exception reaching 9.8%), which indicates that the regression models are adequate to predict these responses, as shown in Table 3.

The optimized condition is also consistent with the microstructural stability observed at calcium chloride concentrations higher than 1% w/v, and the high concentrations of alginate which allow not only to dilute in some extent the effect of Fe^{3+} from the extracts (as mentioned above) at the higher scale (~100 nm), but also to stabilize the structure of the rods observed at the scale ~10 nm, resembling the structure from the parent gels (controls).

Conclusion

In the present research article, extracts from beet by-products were encapsulated in Ca(II)-alginate beads by ionotropic gelation method and optimized through a blocking experimental design with two variables (concentration of sodium alginate and calcium chloride), showing that the best condition is the 1.5% w/v of sodium alginate and 2.5% w/v of calcium chloride. Under these conditions, the highest values for the bioactive properties (TPC, ABTS, and FRAP) are achieved. On the other hand, they decreased as the concentration of sodium alginate is reduced and the same trend occurred in the analyzed macroscopic property, roundness. The microstructural study showed that the structural parameters were explained as a function of sodium alginate concentration more than calcium chloride, as well as the modifications that the extract generates in the alginate network. This manuscript is the first report which combines the optimization of the encapsulation of extracts in Ca(II)-alginate beads with known antioxidant properties during both digestion and fermentation with the evaluation of the microstructural effect at molecular and supramolecular scale. The understanding of the internal structure of the gel matrix, as well as the optimization of the synthesis variables, could allow the modulation of advanced applications in the formulation of functional ingredients.

Declaration of Competing Interests

The authors declare that they have no known competing financial interests or personal relationships that could have appeared to influence the work reported in this paper.

Acknowledgments

This work was supported by the Brazilian Synchrotron Light Laboratory (LNLS, Brazil, proposal SAXS1-20190143 and SAXS1-20190073), Agencia Nacional de Promoción Científica y Tecnológica (ANPCyT PICT-2017-0569), and Consejo Nacional de Investigaciones Científicas y Técnicas (TRAC PhD scholarship).

Supplementary materials

Supplementary material associated with this article can be found, in the online version, at doi:10.1016/j.fhfh.2021.100030.

References

Agüero, L., Zaldivar-Silva, D., Peña, L., & Dias, M. L. (2017). Alginate microparticles as oral colon drug delivery device: A review. *Carbohydrate Polymers, 168*, 32–43.

Aguirre Calvo, T. R., Molino, S., Perullini, M., Rufián-Henares, J. Á., & Santagapita, P. R. (2020a). Effect of in vitro digestion-fermentation of Ca(II)-alginate beads containing sugar and biopolymers over global antioxidant response and short chain fatty acids production. *Food Chemistry, 333*, Article 127483.

Aguirre Calvo, T. R., Molino, S., Perullini, M., Rufián-Henares, J. Á., & Santagapita, P. R. (2020b). Effects of in vitro digestion–fermentation over global antioxidant response and short chain fatty acid production of beet waste extracts in Ca(II)-alginate beads. *Food & Function, 11*, 10645.

Aguirre Calvo, T. R., Perullini, M., & Santagapita, P. R. (2018). Encapsulation of betacyanins and polyphenols extracted from leaves and stems of beetroot in Ca(II)-alginate beads: A structural study. *Journal of Food Engineering, 235*, 32–40.

Aguirre Calvo, T. R., & Santagapita, P. R. (2016). Physicochemical characterization of alginate beads containing sugars and biopolymers. *Journal of Quality and Reliability Engineering* ID:9184039.

Aguirre Calvo, T. R., Santagapita, P. R., & Perullini, M. (2019). In *Functional and structural effects of hydrocolloids on Ca (II)-alginate beads containing bioactive compounds extracted from beetroot: 111* (pp. 520–526). LWT- Food Science and Technology.

Bennacef, C., Desobry-Banon, S., Probst, L., & Desobry, S. (2021). Advances on Alginate use for spherification to encapsulate biomolecules. *Food Hydrocolloids*, Article 106782.

Benzie, I. F. F., & Strain, J. J. (1996). The ferric reducing ability of plasma (FRAP) as a measure of "antioxidant power": The FRAP assay. *Analytical Biochemistry, 239*, 70–76.

Brewer, M. S. (2011). Natural antioxidants: Sources, compounds, mechanisms of action, and potential applications. *Comprehensive Reviews in Food Science and Food Safety, 10*(4), 221–247.

Carley, K. M., Kamneva, N. Y., & Reminga, J. (2004). Response surface methodology. *Wiley Interdisciplinary Reviews: Computational Statistics, 2*(2).

Celli, G. B., Teixeira, A. G., Duke, T. G., & Brooks, M. S. L. (2016). Encapsulation of lycopene from watermelon in calcium-alginate microparticles using an optimised inverse-gelation method by response surface methodology. *International Journal of Food Science & Technology, 51*(6), 1523–1529.

Chan, E. S., Lee, B. B., Ravindra, P., & Poncelet, D. (2009). Prediction models for shape and size of Ca-alginate macrobeads produced through extrusion–dripping method. *Journal of Colloid and Interface Science, 338*(1), 63–72.

Deepak, V., Kalishwaralal, K., Ramkumarpandian, S., Babu, S. V., Senthilkumar, S. R., & Sangiliyandi, G. (2008). Optimization of media composition for Nattokinase production by Bacillus subtilis using response surface methodology. *Bioresource Technology, 99*(17), 8170–8174.

Dodero, A., Pianella, L., Vicini, S., Alloisio, M., Ottonelli, M., & Castellano, M. (2019). Alginate-based hydrogels prepared via ionic gelation: An experimental design approach to predict the crosslinking degree. *European Polymer Journal, 118*, 586–594.

Fang, Z., & Bhandari, B. (2010). Encapsulation of polyphenols–a review. *Trends in Food Science & Technology, 21*(10), 510–523.

Goos, P., & Donev, A. N. (2006). Blocking response surface designs. *Computational Statistics & Data Analysis, 51*(2), 1075–1088.

Ha, B. B., Jo, E. H., Cho, S., & Kim, S. B. (2016). Production optimization of flying fish roe analogs using calcium alginate hydrogel beads. *Fisheries and Aquatic Sciences, 19*(1), 30.

Jeong, C., Kim, S., Lee, C., Cho, S., & Kim, S. B. (2020). Changes in the physical properties of calcium alginate gel beads under a wide range of gelation temperature conditions. *Foods (Basel, Switzerland), 9*(2), 180.

Ji, C., Cho, S., Gu, Y., & Kim, S. (2007). The processing optimization of caviar analogs encapsulated by calcium-alginate gel membranes. *Food Science and Biotechnology, 16*(4), 557–564.

Kaur, N., Singh, B., & Sharma, S. (2018). Hydrogel for potential food application: Effect of sodium alginate and calcium chloride on physical and morphological properties. *The Pharma Innovation Journal, 7*(7), 142–148.

Lee, B. B., Ravindra, P., & Chan, E. S. (2013). Size and shape of calcium alginate beads produced by extrusion dripping. *Chemical Engineering & Technology, 36*(10), 1627–1642.

Llorach, R., Espin, J. C., Tomás-Barberán, F. A., & Ferreres, F. (2003). Valorization of cauliflower (*Brassica oleracea* L. var. *botrytis*) by-products as a source of antioxidant phenolics'. *Journal of Agricultural and Food Chemistry, 51*, 2181–2187.

Najafi-Soulari, S., Shekarchizadeh, H., & Kadivar, M. (2016). Encapsulation optimization of lemon balm antioxidants in calcium alginate hydrogels. *Journal of Biomaterials Science, Polymer edition, 27*(16), 1631–1644.

Narsaiah, K., Jha, S. N., Wilson, R. A., Mandge, H. M., & Manikantan, M. R. (2014). Optimizing microencapsulation of nisin with sodium alginate and guar gum. *Journal of Food Science and Technology, 51*(12), 4054–4059.

Nayak, A. K., Das, B., & Maji, R. (2012). Calcium alginate/gum arabic beads containing glibenclamide: Development and in vitro characterization. *International Journal of Biological Macromolecules, 51*(5), 1070–1078.

Nedovic, V., Kalusevic, A., Manojlovic, V., Levic, S., & Bugarski, B. (2011). An overview of encapsulation technologies for food applications. *Procedia Food Science, 1*, 1806–1815.

Posbeyikian, A., Tubert, E., Bacigalupe, A., Escobar, M. M., Santagapita, P. R., Amodeo, G., et al. (2021). Evaluation of calcium alginate bead formation kinetics: An integrated analysis through light microscopy, rheology and microstructural SAXS. *Carbohydrate Polymers, 269*, Article 118293.

Reis, C. P., Neufeld, R. J., Vilela, S., Ribeiro, A. J., & Veiga, F. (2006). Review and current status of emulsion/dispersion technology using an internal gelation process for the design of alginate particles. *Journal of Microencapsulation, 23*(3), 245–257.

Rijo, P., Falé, P. L., Serralheiro, M. L., Simões, M. F., Gomes, A., & Reis, C. (2014). Optimization of medicinal plant extraction methods and their encapsulation through extrusion technology. *Measurement, 58*, 249–255.

Shrikhande, A. J. (2000). Wine by-products with health benefits. *Food Research International, 33*, 469–474.

Sonego, J. M., Santagapita, P. R., Perullini, M., & Jobbágy, M. (2016). Ca (II) and Ce (III) homogeneous alginate hydrogels from the parent alginic acid precursor: A structural study. *Dalton Transactions, 45*(24), 10050–10057.

Stojanovic, R., Belscak-Cvitanovic, A., Manojlovic, V., Komes, D., Nedovic, V., & Bugarski, B. (2012). Encapsulation of thyme (Thymus serpyllum L.) aqueous extract in calcium alginate beads. *Journal of the Science of Food and Agriculture, 92*(3), 685–696.

Šumić, Z., Vakula, A., Tepić, A., Čakarević, J., Vitas, J., & Pavlić, B. (2016). Modeling and optimization of red currants vacuum drying process by response surface methodology (RSM). *Food Chemistry, 203*, 465–475.

Traffano-Schiffo, M. V., Aguirre Calvo, T. R., Castro-Giraldez, M., Fito, P. J., & Santagapita, P. R. (2017). Alginate beads containing lactase: Stability and microstructure. *Biomacromolecules, 18*(6), 1785–1792.

Traffano-Schiffo, M. V., Calvo, T. R. A., Avanza, M. V., & Santagapita, P. R. (2020). High-intensity ultrasound-assisted extraction of phenolic compounds from cowpea pods and its encapsulation in hydrogels. *Heliyon, 6*(7), e04410.

Traffano-Schiffo, M. V., Castro-Giraldez, M., Fito, P. J., Perullini, M., & Santagapita, P. R. (2018). Gums induced microstructure stability in Ca(II)-alginate beads containing lactase analyzed by SAXS. *Carbohydrate Polymers, 179*, 402–407.

Velasco, C., Beh, E. J., Le, T., & Marmolejo-Ramos, F. (2018). The shapes associated with the concept of 'sweet and sour' foods. *Food Quality and Preference, 68*, 250–257.

Wootton-Beard, P. C., & Ryan, L. (2011). A beetroot juice shot is a significant and convenient source of bioaccessible antioxidants. *Journal of Functional Foods, 3*(4), 329–334.

Zazzali, I., Aguirre Calvo, T. R., Ruíz-Henestrosa, V. M. P., Santagapita, P. R., & Perullini, M. (2019). Effects of pH, extrusion tip size and storage protocol on the structural properties of Ca (II)-alginate beads. *Carbohydrate Polymers, 206*, 749–756.

United Nations (2021). The 17 goals. Department of Economic and Social Affairs. Retrieved from https://sdgs.un.org/goals. Accessed April 21, 2021.